In situ TEM observations of fast grain-boundary motion in stressed nanocrystalline aluminum films

Marc Legros [a,*], Daniel S. Gianola [b], Kevin J. Hemker [b]

[a] *CEMES-CNRS, 29 rue J. Marvig, 31055 Toulouse, France*
[b] *Mechanical Engineering, Johns Hopkins University, Baltimore, MD 21218, USA*

Abstract

Free-standing nanocrystalline Al thin films have been strained in situ in a transmission electron microscope at room-temperature. Extensive grain-boundary migration accompanies the in situ loading and has been observed to occur preferentially at crack tips and only in the presence of the applied stress. This grain growth precedes dislocation activity, and measured boundary velocities are greater than can be explained by diffusive processes. The unambiguous observations of stress-assisted grain growth are compatible with recently proposed models for stress-coupled grain-boundary migration. The growth occurs in a faceted manner indicative of preferential boundaries. The fast collapse of small grains with sizes of 30–50 nm demonstrates the unstable nature of a nanocrystalline structure. Clearly observable shape changes testify to the effectiveness of grain-boundary migration as a deformation mechanism, and preferential grain growth at crack tips resulted in efficient crack tip blunting, which is expected to improve the films' fracture toughness.
© 2008 Acta Materialia Inc. Published by Elsevier Ltd. All rights reserved.

Keywords: In situ transmission electron microscopy (TEM); Grain-boundary migration; Nanocrystalline film; Aluminum

1. Introduction

Room-temperature plasticity in polycrystalline metals and alloys is commonly understood and modeled in terms of dislocation nucleation, mobility, and interaction with various obstacles. For metals and alloys, the primary role of grain boundaries is thought to be that of obstacles to dislocation motion, and the widely referenced Hall–Petch relation [1,2] predicts that decreasing the average grain size, effectively increasing the density of grain boundaries, results in increased strength. This relation has been shown to hold for a wide range of materials and grain sizes, and considerable interest has been placed on extrapolating this relationship to the nanocrystalline regime. There is clear evidence to indicate that the strength of nanocrystalline metals falls short of Hall–Petch predictions at the smallest grains sizes (below 100 nm) [3–6]. This realization and the

observation that nanocrystalline metals do possess at least moderate levels of ductility have led the community to consider alternative deformation mechanisms. Proposed alternative room-temperature deformation mechanisms of nanocrystalline metals have included: grain-boundary sliding [7], grain rotation [8,9], diffusional creep [10,11], grain-boundary migration, dislocation nucleation or absorption at grain boundaries [12–16] and enhanced partial dislocation activity [17–22]. The focus of this manuscript is on the motion of grain boundaries (GBs).

At variance from dislocation plasticity, GB-mediated plasticity occurs mainly through diffusive processes. In coarse-grained or microcrystalline materials, GB migration and Coble creep are temperature-dependent and related to the diffusion of atoms across or along the grain-boundary. Diffusion-induced grain-boundary migration (DIGM) has been observed in a number of materials and is a mechanism that applies to all types of grain boundaries. DIGM has been widely studied [23–25] and requires a driving force that derives from a difference in free energy on either side

---

of a GB. This energy difference can arise from several factors such as solute concentration, GB surface tension (curvature), or non-uniform stress states. Balluffi and Cahn [25] proposed a mechanism for DIGM in which differences in the diffusion coefficients of the diffusing species along the GBs cause a self-sustaining climb of grain-boundary dislocations and motion of the associated GB steps. Other mechanisms and driving forces that have been used to describe diffusion-related GB motion include: Coble creep [10], which is only effective at high temperatures [26] in large-grained polycrystals; reduction in the number and curvature of GBs through homogeneous grain growth [27]; and local shuffling of atoms between the GB and the adjacent grains (short-range diffusion process) [28]. The last process is based on in situ TEM experiments [29] showing defect-free jerky GB migration and is described in detail by Babcock and Balluffi in [30]. The idea is that it is energetically favorable, as shown for a Σ5 boundary, to displace atoms by shuffling over very short distances in each unit cell of the GB.

GB migration can also be carried out by athermal shear, without diffusion. This is predictable when the misorientation between two grains is small, as in the case of low-angle tilt boundaries that can be described as discrete networks of dislocations [31]. The low-temperature displacement of a low-angle GB thus results from the glide of this dislocation array. This has been demonstrated experimentally in Al polycrystals under creep conditions at 200 °C [32] and for Al bicrystals [33]. Traditionally this mechanism is envisaged to operate for a low-angle GB, but recent theoretical descriptions by Cahn and colleagues [34,35], molecular dynamics (MD) [36,37] simulations and experimental observations [38–40] have shown that stress-coupled grain-boundary migration operates for high-angle grain tilt boundaries as well. The perpendicular motion of both low- and high-angle GBs can be framed in terms of their dislocation structure, as determined by the Frank–Bilby equation. The coupling between the applied shear stress and the GB motion, either positive or negative, can result in potential back-and-forth motion of the GB. As shown by MD, the change in shear stress/motion coupling can be attributed to a change in the dislocation structure of the GB during the movement. This entirely geometric model is very effective at predicting the results obtained from MD, but both approaches are employed on relatively simple, planar, GBs.

Despite obvious fundamental differences between diffusion-based and stress-coupled GB motion, experimental attempts to separate both mechanisms has proven elusive. For example, high-temperature measurement of GB motion in Al bicrystals leads to displacements predicted by the shear coupling GB model [33], but migration energies (E_m) are very similar to those found for DIGM [40]. In fact, E_m, determined from the GB mobility [38,41,42], seems to depend more on its structure [43–45] than on its mode of motion. Attempts to quantify GB mobility are also complicated by the fact that GB structures can change and evolve as they migrate, as evidenced by observations of dislocation emission and absorption during GB migration experiments [46–49]. There is also no clear relationship between the GB energy (E_{GB}) and the grain-boundary migration energy. Plotting E_m as a function of GB characters shows a sharp transition between low- and high-angle GB motion. Typically, E_m for low-angle GBs has been reported to be close to the activation energy for bulk diffusion, while that for high-angle GBs is closer to the activation energy for diffusion along grain boundaries. Although well documented, this low-to-high angle transition is not fully understood [39]. The situation becomes even more complex in polycrystalline materials, where E_m differs significantly from bicrystals [46,50] because of multiple junctions [51]. In real polycrystals, GBs are also not predominantly pure twist or tilt character, and GB migration cannot be conservative and requires diffusion and climb of the various GB dislocations.

In nanocrystalline materials, the influence of GB migration is expected to be critical for several reasons: the small grain size and associated GB curvature increase the stored energy, the high density of GBs and vacancies coupled with reduced diffusion pathways accelerates diffusive processes, and dislocation-mediated plasticity demands much higher stresses. Recent MD simulations suggest that dislocation-mediated plasticity never completely disappears [52] but that the role of stress-assisted GB deformation is increased at nanocrystalline grain sizes. MD simulations suggest that GB deformation can occur by GB sliding [53,54] or by a Coble creep-like diffusive process involving grain growth and coalescence [55,56]. A few authors also consider atoms in high-energy GBs to be very close to their melted state, making the migration of these GBs easier, for instance by atomic shuffling [57]. The possibility of stress-coupled GB motion [35] offers yet another possibility for GB-related plasticity but is yet to be established for a general population of grain boundaries and in the specific case of nanocrystalline metals.

Clean experimental observations of GB sliding and grain rotation in nanocrystalline metals have proven tenuous and evidence in support of these mechanisms remains controversial [9,58–60], mainly because it is extremely challenging to image individual and adjacent nanocrystalline grains with conventional in situ TEM. By contrast, the observed growth of nanocrystalline grains by post mortem TEM observations of specimens that have been subjected to an applied stress, through indentation [61–63] or uniaxial loading [64,65], has been clearly documented. Tensile testing of nanocrystalline specimens has proved to be challenging, but testing very small specimens also provides a way to bypass the inherent residual porosity of many nanocrystalline samples [66–68]. Recent advances in micro-tensile testing [3,69,70] allows one to determine the stress–strain response of tiny samples and free-standing films. By coupling micro-tensile thin film testing, in situ synchrotron diffraction experiments and post mortem TEM, Gianola and co-workers recently established grain growth as an active deformation mode in abnormally ductile nc-Al thin films at room-temperature [71]. Moreover, by varying the applied strain-rate during testing, it was

shown that the stress, not the total plastic strain, discriminated the amount of grain growth that was seen [72]. The importance of the stress was reinforced by compressive experiments on nanocrystalline Cu, where enhanced grain growth was observed proceeding both deformation at cryogenic temperatures [73] and stress-controlled transient experiments [74].

This observation of discontinuous grain growth as a low-temperature deformation mechanism for nanocrystalline Al appears, in many ways, to be related to the phenomenon of stress-assisted grain-boundary migration recently described [36,37]. There are, however, many outstanding questions about the fundamental mechanisms responsible for this grain growth. Is it stress-driven or strain-driven? Is dislocation-based plasticity necessary to trigger grain growth? Are certain GBs favored for migration or do they all move at the some rate? Is overall grain growth homogeneous or heterogeneous? How do the kinetics of GB migration play out? Direct observations and measurements of GB velocities under simple loading conditions are needed to answer these questions and in situ tensile testing in a TEM provides such capability. Here, we report on in situ TEM experiments that were performed using the same nanocrystalline Al films deformed "macroscopically" by Gianola et al. [71]. The motivation for this study was an interest in garnering insight about the grain growth that occurs in these films and in addressing, to the extent possible, many of these outstanding questions. The focus of this study is on GB events rather than fine intragranular dislocation processes, but we have attempted to monitor both GB and dislocation activity for comparative purposes.

2. Experimental procedure

Al thin films of different thicknesses were sputter-deposited on Si wafers with interrupted cycles to prevent colum-nar growth. In the current study, 380 and 180 nm thick films have been tested. The average grain sizes for these films were 90 and 40 nm, respectively, which means that, on average, 4–5 grains are found in the through thickness of the foils. This final point was confirmed by measurements of grain sizes from cross-sectional TEM images, giving a mean aspect ratio (unity being equiaxed and $\gg 1$ being columnar) of 1.4 ± 0.8. The films were patterned using standard lift-off photolithography and micro-tensile specimens and rectangular strips were released from the underlying Si substrate with a gaseous xenon difluoride dry etch. Details about the film deposition, processing and lift-off techniques employed for this study are given in Refs. [68,71].

The tensile foils used for in situ TEM tensile testing were typically 3 mm long and 0.5–1 mm wide. They were glued onto deformable Cu grids with cyanocrylate or epoxy glue (see Fig. 1a) and tested within 24 h. Dots of silver paint were added between the Cu grid and the nc-Al film to ensure electrical contact and prevent beam charging. Films were strained at 300 K in a JEOL 2010, operating at 200 kV. Various imaging conditions were employed and conventional bright field (BF) and dark field (DF) images were recorded. The displacement rate of the mobile jaw on the Gatan straining holder was set to 100–500 nm s^{-1}. Pulses of approximately 1 s were applied after which the grips were fixed and relaxation processes where observed. Initial motion of the grips typically resulted in the following sequence: rigid body motion and grip adjustments; flattening of the foils which was monitored using bend contours; elastic loading and plastic loading. In the plastic regime, micro- (nano-)structural changes were observed to occur concurrently with the application of strain. Grain-to-grain contrast differences facilitated direct observations of grain growth, and when present intragranular dislocation activity was easily identified by fast changes in the residual
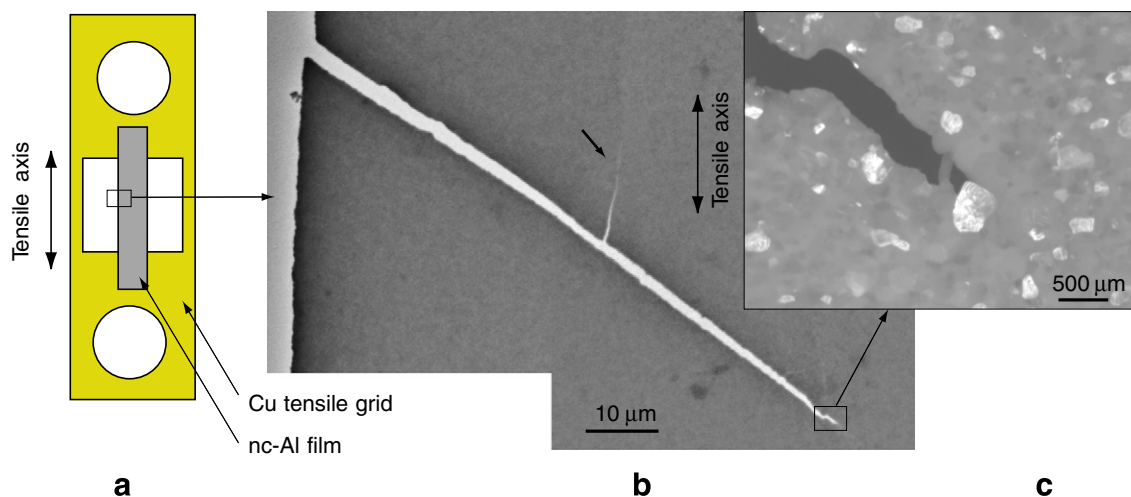

Fig. 1. (a) Sketch of a free-standing nc-Al film on a deformable Cu grid; (b) bright field (BF) and (c) dark field (DF) micrographs showing a 100 μm crack in a 380 nm thick nc-Al film prior to deformation. The enlarged view (c) indicates that the initial grain size and microstructure is preserved except for the one grain located at the very tip of the crack. The short arrow indicates a secondary crack that did not expand during straining. The tensile axis is vertical, as in all the micrographs presented in this study (otherwise mentioned).

contrast, even for conditions of $\boldsymbol{g} \cdot \boldsymbol{b} = 0$ ($\boldsymbol{g}$ being the diffraction vector used to form the image and $\boldsymbol{b}$ the Burgers vector of the dislocation).

In the experiments conducted in this study, plastic deformation always occurred preferentially at the tip of pre-existing cracks, which were probably introduced during foil preparation. The presence of these cracks was fortuitous but greatly aided the study by localizing the activity and providing valuable insight as to where to look for microstructural changes. Because of this configuration, alignment of the foil on the Cu grid was not critical since the stress tensor was primarily determined by the crack geometry. Nevertheless, the cracks were loaded in a predominately mode-I configuration. The majority of images for this study were taken in dark field (DF) conditions. These conditions were set, prior to plastic deformation, by defining five positions for the objective aperture, each of which centered on a distinct diffraction spot on the 1 1 1 diffraction ring acquired at the beginning of the experiment. The optimum imaging

conditions were found by dynamically switching between these five positions and adjusting the double-tilt specimen stage during the in situ experiments.

3. Experimental results

Fig. 1 presents the typical set up and as-deposited nanostructure of a 380 nm thick (90 nm initial grain size) Al film before in situ straining. Fig. 1a is a sketch of the nc-Al film strip glued on a stretchable Cu grid. Fig 1b is a low magnification micrograph of the side of the film that has been cracked during its manipulation and gluing. The crack tips that were observed in this study did not change the initial grain size or microstructure except for the one or two grains in contact with the tip that were always found to be larger than the initial average grain size. This can be seen in Fig. 1c, which is an enlargement of the crack tip from Fig. 1b. The tensile axis is aligned along vertical in all micrographs (unless otherwise mentioned), but the
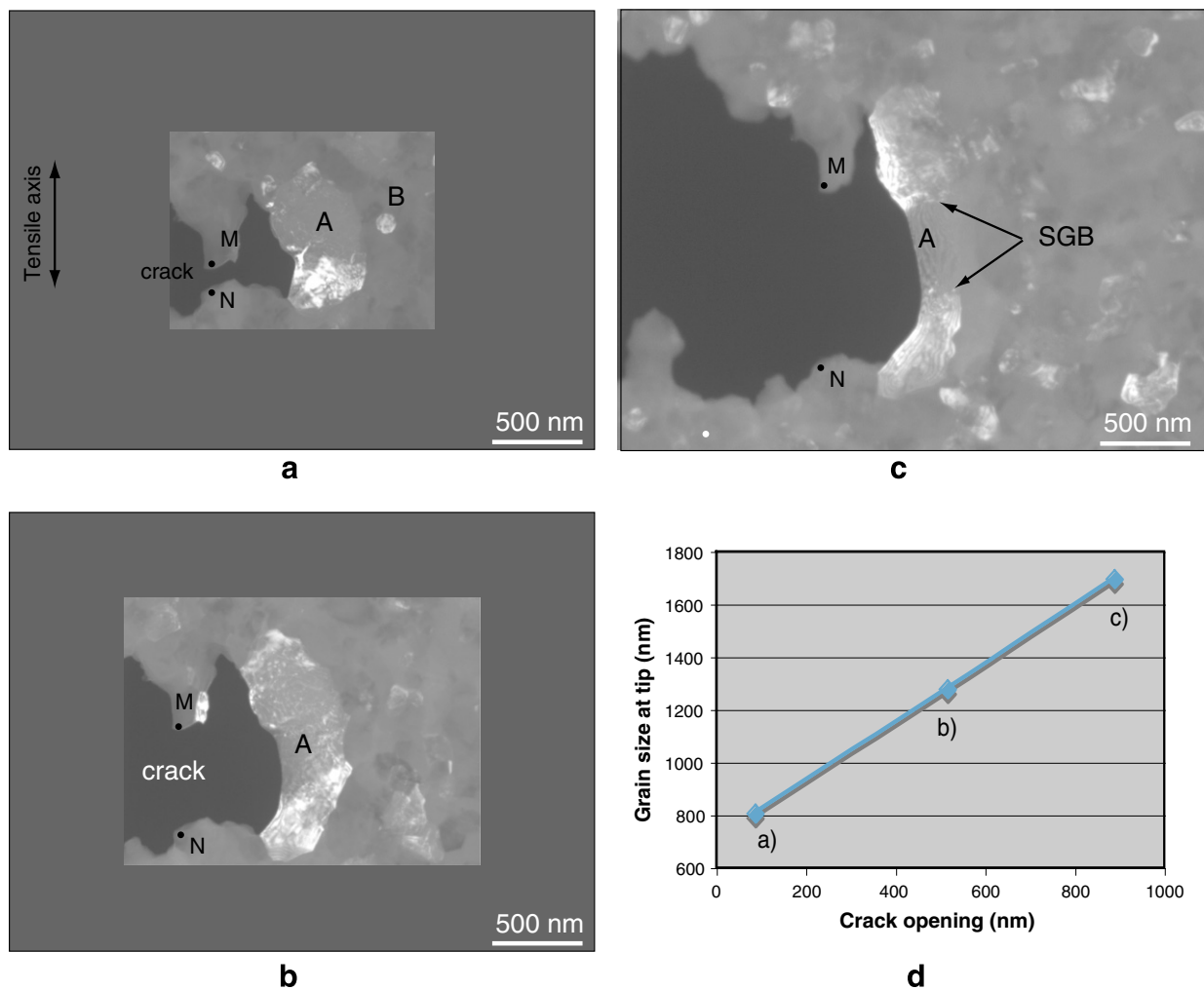

Fig. 2. (a–c) Dark field micrographs taken with the same $\boldsymbol{g}$ vector during an in situ TEM tensile experiment on a 180 nm thick Al film. M and N are fixed points across the crack. Grain A is stretched as the crack opens. Grey frames were added to maintain the same scale bar and demonstrate the elongation (up to 300% here) undergone by A. Grain length against crack opening is plotted in (d); the error bars are about 50 nm, smaller than the diamond-shaped symbols.

stress state in the foil is dominated by the stress concentration at the tip of the crack.

When a tensile stress was applied to the nc-Al foils, pronounced grain growth was observed to occur at the crack tip, as is shown in the sequence given in Fig. 2. This figure is composed of three still images that were taken during an in situ TEM experiment. The graph at the bottom of the figure gives the length of grain A as a function of the crack opening, which was measured as the distance between two points M and N. The initial configuration of this sample was similar to that described in Fig. 1, and Fig. 2a shows that grain A, which is located right at the crack tip, had undergone substantial grain growth prior to the in situ experiment. We assume that this growth occurred as a result of crack tip stresses associated with the handling of the thin foil and note that the small grain (B) positioned adjacent to A remains in the nanometer scale. The time intervals between Fig. 2a–c are 25 and 18 min, respectively, while a macroscopic displacement of 10 μm was applied with the straining holder. Grain growth was observed to occur predominantly at the crack tip. This growth was extensive and was not limited by the film thickness. See for example grain A, which elongates as the crack opens and completely bridges and blunts this crack.

We have observed that, under stress, dislocation activity is important in grains that are larger than 200 nm. Extensive dislocation activity was observed in grain A and as dislocation-based plasticity continued to operate, classical work-hardening processes, such as dislocation tangling, take place and lead to the formation of cells and subgrains. Subgrain boundaries (SGB) are highlighted in Fig. 2c. For this particular grain (A), it is worth noting that the length of the grain scales with the imposed displacement of the crack tip, as measured between the two markers M and N. As shown in Fig. 2d, the line describing this relation intersects the *y*-axis at approximately 700 nm, which indicates that a primary grain growth occurred at zero displacement; that is, under the influence of the stress field only. Further examples
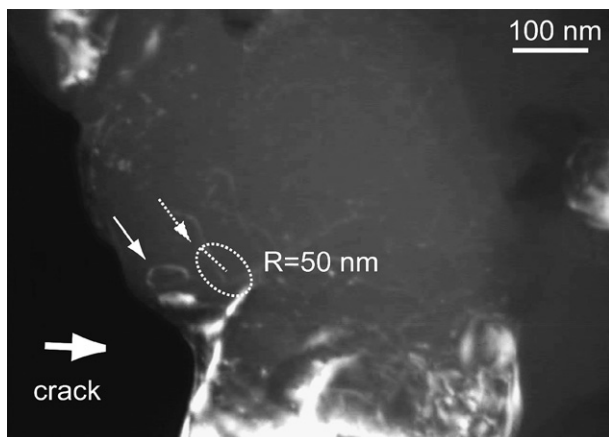

Fig. 3. Video frame captured during an in situ experiment showing an expanding dislocation loop (plain arrow) in a large grain located at the crack tip. The dashed ellipse represents the projected dislocation loop and its radius in the glide plane.

of grain growth that is stress-assisted and not strain-assisted will be given later (Figs. 5 and 6).

These initial observations emphasize the fact that microstructural evolution only occurs in a highly localized region at the crack tip. Dislocation activity was observed a bit further away, but detectable grain growth was only seen for the 3–5 grains that were in direct contact with the crack tip. To estimate the stress in this region, we have measured a few dislocation loops that were expanding under the applied stress in grown grains right at the crack tip. Fig. 3 is a dark field video capture of such a loop right before it moves during an in situ test. On the left, a thick arrow points to the developing crack. The dashed ellipse drawn next to the expanding loop corresponds to the radius of curvature of this loop projected in the dislocation glide plane. We have assumed that its Burgers vector b is $a/2 <110>$. From the radius of curvature R and using the Orowan equation, we can then estimate that the local stress σ has to be larger than the dislocation line tension τ

$$\sigma > \tau = \frac{\mu b}{R} \tag{1}$$

where μ is the shear modulus of aluminum (26 GPa) and b is assumed to be the magnitude of an $a/2 <110>$ dislocation (0.286 nm). A radius of curvature of 50 nm leads to a resolved shear stress of 150 MPa, which corresponds to an applied stress larger than 300 MPa, assuming an optimum Schmid factor of 0.5.

Fig. 4 is a series of pictures extracted from a long video sequence representing the most common grain growth mechanism and speed encountered in this study. Grains A and B were monitored over 10 min while under stress. Grain A is directly in contact with the opening crack tip and the zone between A and B is highly stressed. Grains A and B are faceted in Fig. 4a and may not be in their as-deposited state; rounded grains were observed more frequently in as-deposited films. Nevertheless, grain growth was observed to occur by the displacement of the oppositely facing grain boundaries of A and B, which eventually leads to their contact in Fig. 4e. The grain (C) between grains A and B becomes visible between Fig. 4c and d, although the imaging conditions have not changed (same g). This suggests that the smaller grain (C), which is less than 100 nm, has rotated to align its orientation with those of grains A and B. As the grains A and B grow towards each other, grain C shrinks (Fig. 4d and e) before finally disappearing after approximately 100 s (not shown). From typical sequences like this, we can determine the "average" grain-boundary displacement rate during the in situ experiments. In the example given in Fig. 4 it ranges from 0.1 (grain A) to 0.2 nm s^{-1} (grain B). This migration speed was only observed for GBs that are very close to the crack tip and in the highly stressed region of the sample. Although not quantified, qualitative observations indicate that the grain sizes in these films decreases as one moves away from the crack tip, which is an indication that GB velocity decreases accordingly.
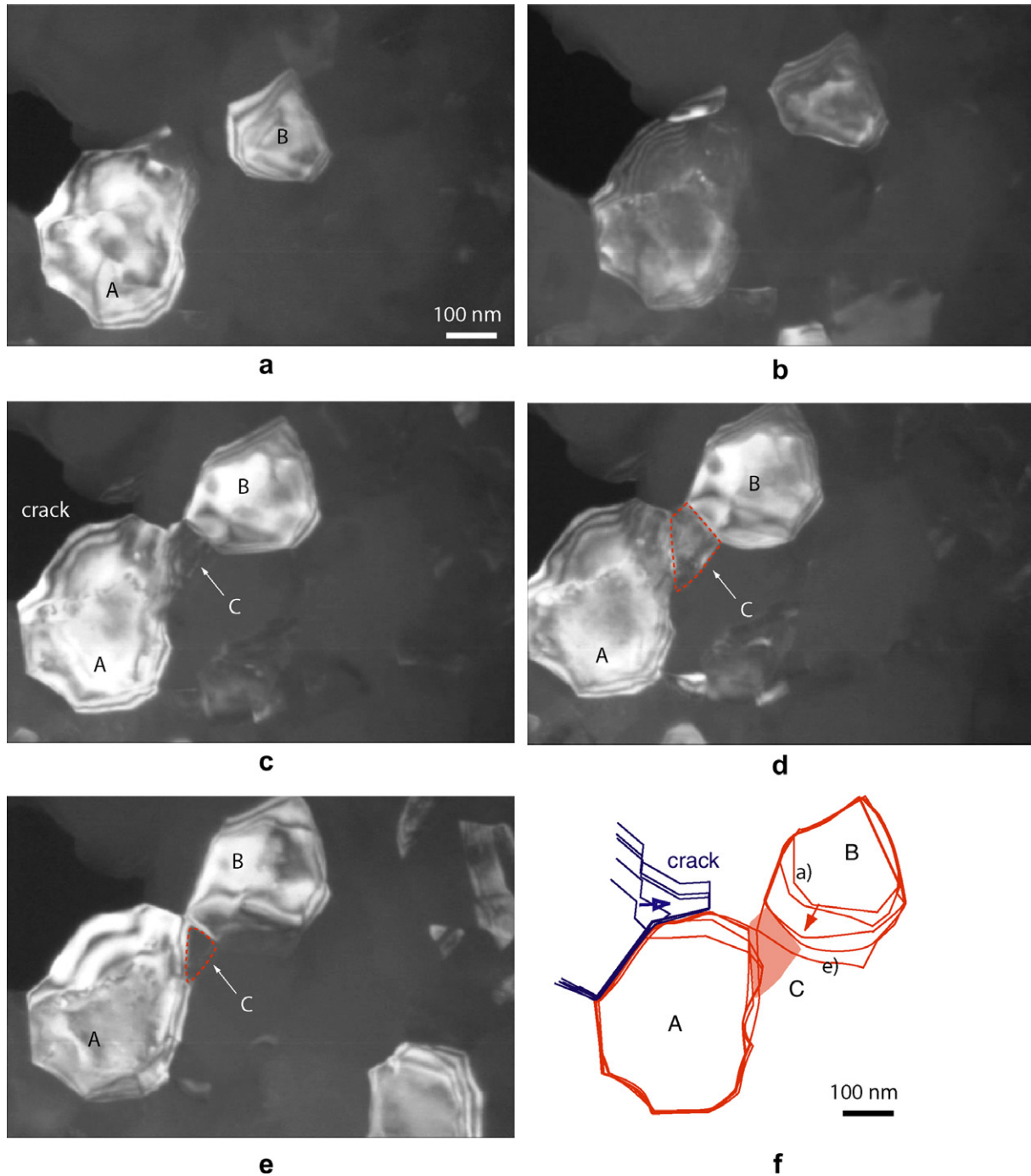
Fig. 4. Video sequence taken in dark field at 300 K. "Regular" grain growth ahead of a crack tip. (a) 0 s, (b) 198 s, (c) 399 s, (d) 497 s, (e) 584 s, and (f) grain growth steps from (a) to (e).

This GB velocity can, in particular cases, reach extremely high values, as described in Fig. 5, where the time scale is much shorter than for Fig. 4. As in the previous example, grains A and B are located ahead of the crack (which is coming from the right in this experiment). These grains had already grown to be 200–300 nm and significant dislocation activity had already taken place (dislocation loops and segments are visible in grains A and B) when this sequence was shot. Close inspection indicates that grains A and B were not connected in the beginning of this sequence (Fig. 5a). Growth and coalescence was initiated by the motion of the lower right part of grain A towards grain B (Fig. 5a–c) at a rate of 5–10 nm s^{-1} (8 nm s^{-1} between Fig. 5a and b). This motion continued until reaching the position of Fig. 5c, where grain A touches and connects with B. In Fig. 5c–e, the upper part of the migrating GB moves very quickly towards grain B. These "jumps" occur over rather large distances (20 and 16 nm), and involve a
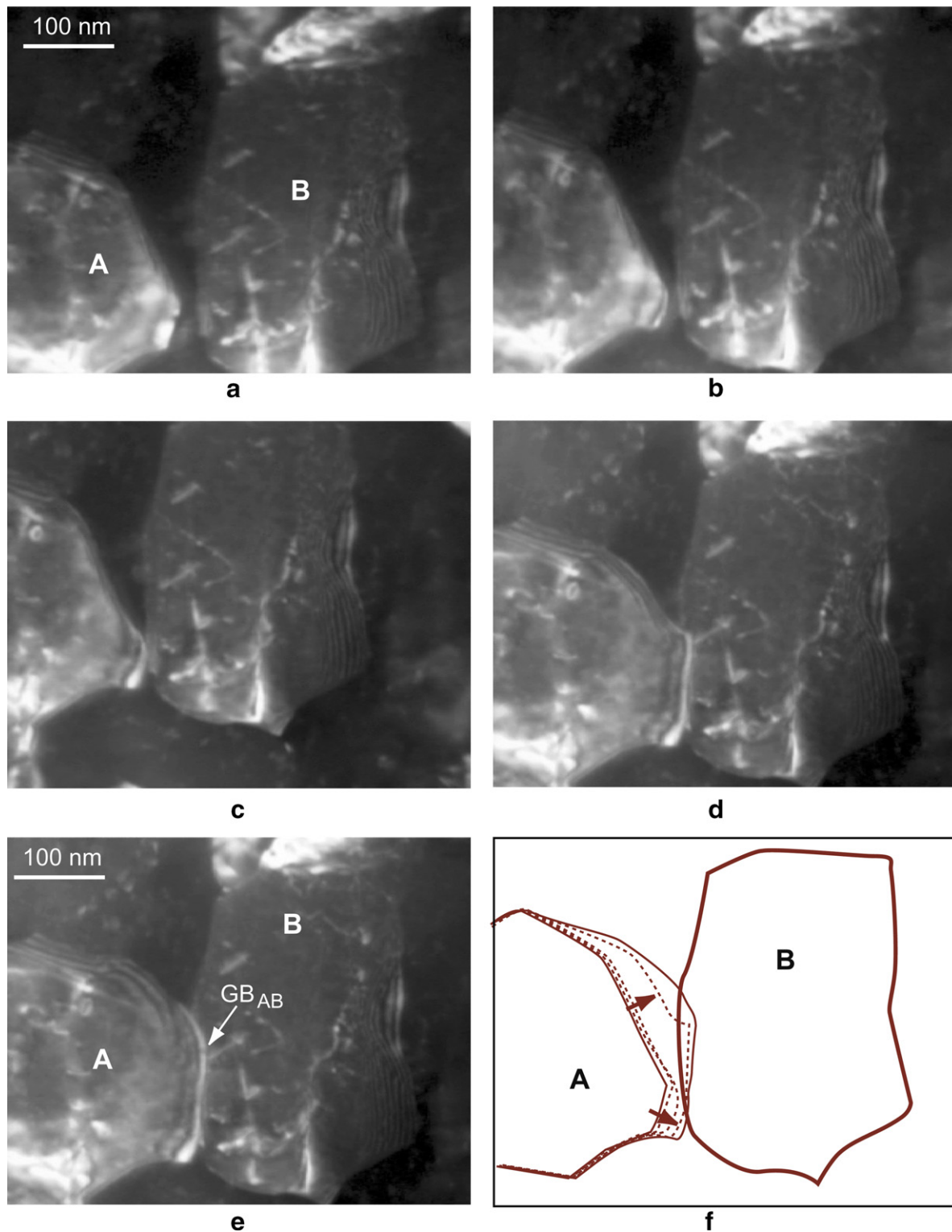
Fig. 5. Grain growth occurring by fast GB motion at 300 K. (a) $t = 0$ s, (b) 1.2 s, (c) 18.16 s, (d) 29.04 s, (e) 29.24 s, and (f) sketch of the successive positions of the GB.

large portion of the GB. The normal velocity between Fig. 5d and e was estimated to be 50 nm s^{-1}. In Fig. 5d, grains A and B have a common boundary (GB$_{AB}$) that is more than 130 nm long and has been created in less than 10 s. Because the sequence was shot in dark field, it was not possible to image and analyze the simultaneous disappearance of the grain that was between A and B (see grain C in Fig. 4 or Fig. 8). It is, however, important to note that the growth of grains A and B and the creation of GB$_{AB}$ did not involve any dislocation emission towards the interior of
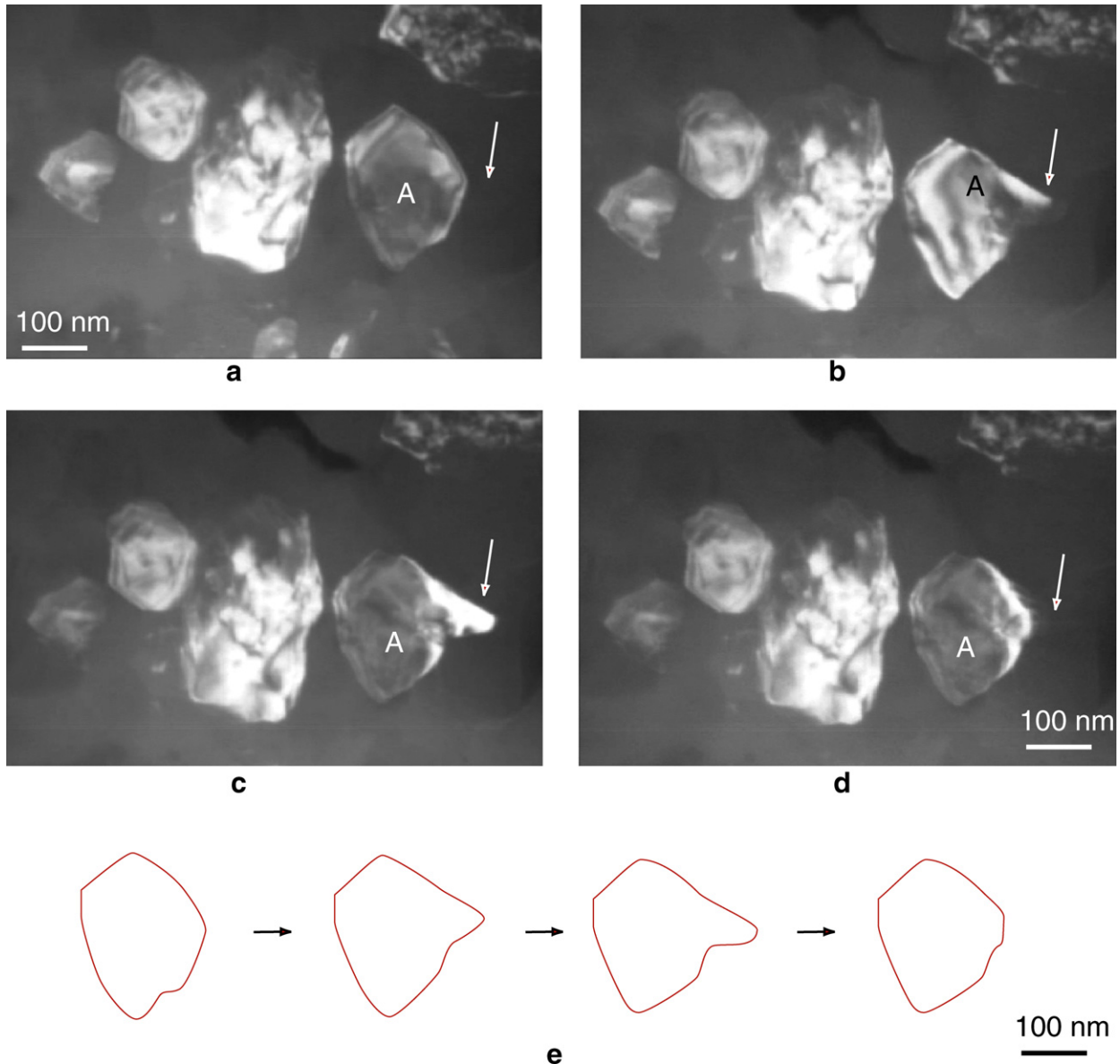
Fig. 6. Back-and-forth motion of a GB portion under a tensile stress. (a) $t = 0$ s, (b) 248 s, (c) 343 s, (d) 346 s, (e) 513 s, and (f) sketch of the grain shape evolution from (a) to (e).

grains A or B or the appearance of a linear defect in the fringe contrast of the GBs. The reverse motion of a portion of GB_{AB} was observed in the video frames that follow this sequence but is not shown here as this phenomenon is better exemplified in Fig. 6. Compared to the observation in Fig. 4, the GB velocity in Fig. 5 is 20–500 higher, suggesting a possible different underlying mechanism for GB migration.

Fig. 6 illustrates the phenomenon of the back-and-forth motion of a GB under a constantly positive stress. The crack tip, coming from the upper left, broadens between Fig. 6b and c. In the sequence from Fig. 6a–c, grain A is observed to grow locally by the motion of the upper right portion to the right (highlighted by white arrows). The tip of this "nose" was observed to move a distance of 80 nm in approximately 360 s, which indicates an average velocity

0.2 nm s^{-1}, comparable to the velocity calculated in Fig. 4. From Fig. 6b–d, there is almost no change in the surrounding microstructure nor in the tensile stress applied, as attested by the constant contrast of the other grains on the left.

Surprisingly, the grain protrusion that was created between 6b and c is erased by the rapid retraction of the GB (Fig. 6c and d). In Fig. 6d grain A has returned to a configuration that is close to what it was in Fig. 6a. The local speed of grain-boundary motion between Fig. 6c and d was estimated to be 30 nm s^{-1}, which is 100 times faster that in the left-to-right motion (Fig. 6a–c) and comparable to the speed calculated in Fig. 5. During this sequence, grain A has been partially sheared by less than five dislocations (dislocations in contrast or in residual contrast), which cannot account for the change of shape of

grain A. This sequence, summarized in Fig. 6e, demonstrates not only that GB motion can occur at different speed under a comparable stress, but also that the direction of motion can be reversed without reversing the applied stress.

The in situ observations represented in Figs. 5 and 6, like those in Fig. 2, indicate that the grain growth does not scale with crack opening displacement and is therefore not directly related to the strain in the specimen. The in situ observations also indicate that grain growth can occur by the coalescence of closely oriented grains, as shown in Fig. 7. In this figure, grains A and B are in an area of high stress at the tip of a crack that is coming from the left. These grains have an apparent size of 180×100 nm and 130×100 nm, respectively, which is close to the initial grain size (90 nm) that was measured for this 380 nm thick
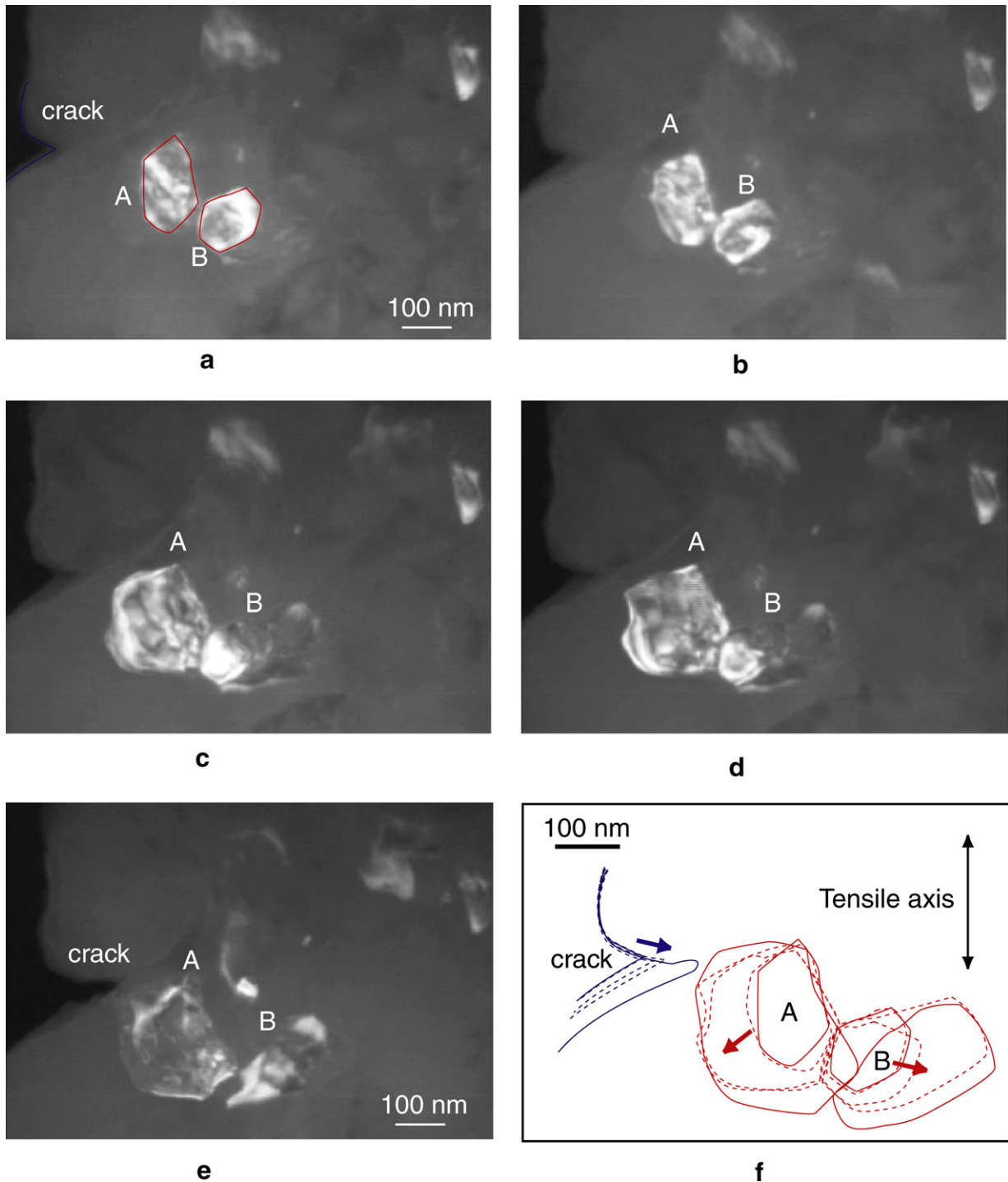

Fig. 7. Growth by re-orientation and coalescence of grains. (a) $t = 0$ s (b) 6 s, (c) 20 s, (d) 22 s, (e) 49 s, and (f) sketch of the grain shape evolution from (a) to (e).
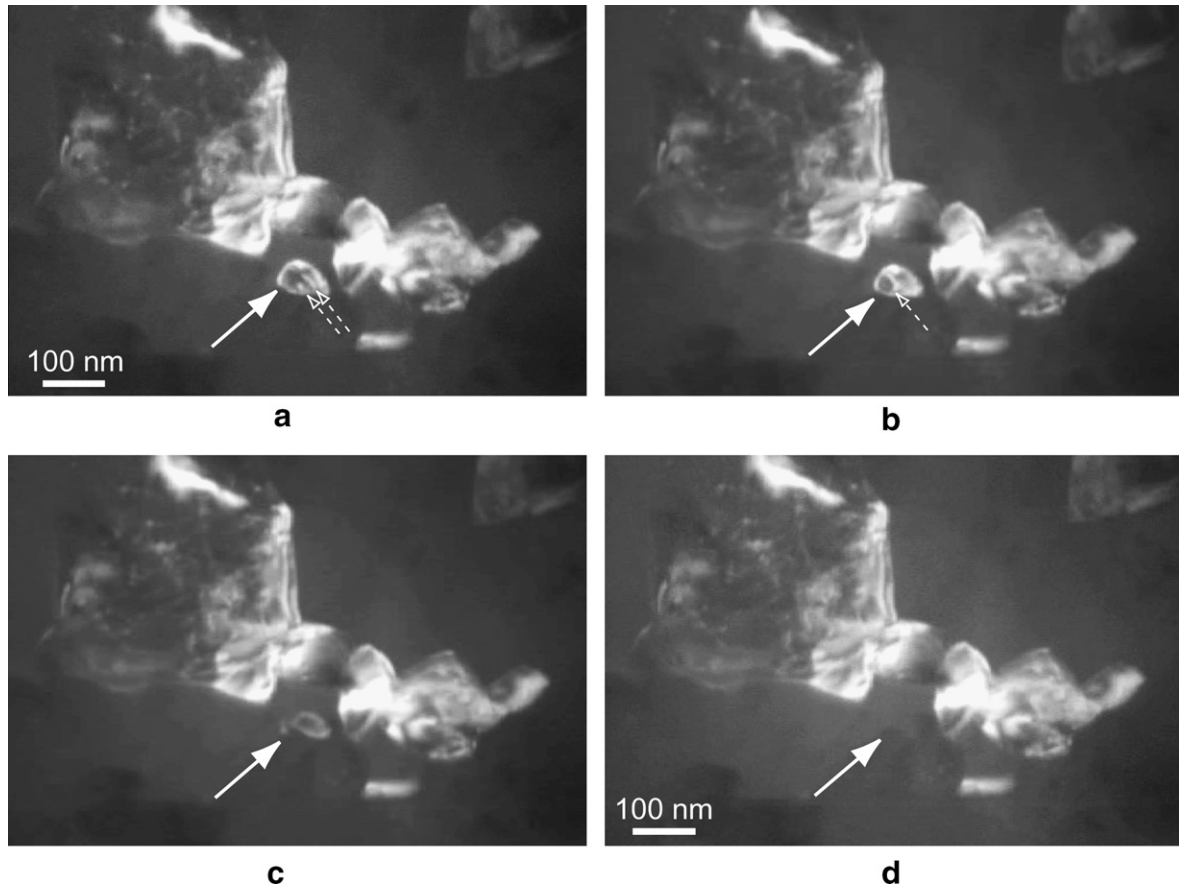
Fig. 8. Disappearance of a grain under stress. (a) $t = 0$ s, (b) 5 s, (c) 7.64 s, (d) 7.76 ns. Note the dislocations loops inside the grain in (b) (dashed arrows) and the remaining dislocation in (c) (dashed arrow). The large arrow shows the disappearing grain and can be considered as a fixed point.

film. The images shown in Fig. 7a–e illustrate that both grains (A and B) double their size in less than one minute. The mechanism for the grain growth is, however, fundamentally different from what was observed in the previous examples. The fact that both grain are visible and have the same contrast in the dark field images indicates that the orientation of this grains was very similar. The combination of these grains during this in situ experiment has been taken as a clear example of grain rotation and coalescence.

The preferential growth of some grains must necessarily mean that other grains are shrinking. The shrinkage and disappearance of small grains has been observed on numerous occasions Fig. 8 is an example of such an event; the grain highlighted by the arrow is 83×57 nm large and contains two dislocation segments that are noted by the dashed arrows. This grain maintained a constant size (Fig. 8a) under load for approximately 1 min and then started to shrink (Fig. 8b). At this time, the dislocation segment on the right moves towards and joins its neighbor to form a loop, which is visible in the middle of the grain in Fig. 8b. This loop was observed to move to the left in a direction opposite what would be predicted by its curvature and is absorbed into the GB that is advancing from left to right. In Fig. 8c, the grain is reduced to a size of 50×36 nm and no longer contains the dislocation loop.

At this point, the grain was observed to collapse in less than 0.12 s (three video frames), which correspond to a GB velocity greater than 200 nm s^{-1}. This rapid collapse of grains smaller than 30–50 nm has been observed on multiple occasions, which suggests a possible minimum grain size under which the applied stress renders the grains unstable.

Additional in situ experiments, not shown here, involved heating cross-sectional wedges of the same nc-Al films while they were still attached to their substrate. No appreciable grain growth was observed and the micro-(nano-)structure of the nc-Al film proved to be very stable up to 723 K. As compared with the in situ observations outlined in this paper, the microstructural stability of the thermally cycled films points to the importance of stress in driving the grain growth observed in this study. The fact that finite thermal stresses arise from the coefficient of thermal expansion (CTE) mismatch between the Al films and Si substrate points to the existence of a critical stress for grain growth.

4. Discussion of results

Most studies on the mechanical behavior of nanocrystalline metals have focused on extension of the Hall–Petch

relation to smaller grain sizes and identification of the deformation mechanism or mechanisms that become operative when microcrystalline plasticity is abated. There is generally acceptance that conventional dislocation mechanisms are inhibited at grain sizes below 100 nm, and MD simulations suggest that below 100 nm and down to 10–20 nm, plastic deformation is accommodated through grain-boundary sliding and the emission of unit and partial dislocations that traverse the grain and are absorbed into the opposite grain-boundary without multiplying or interacting with other dislocations [3]. The prediction of partial dislocation emission is supported by TEM observations of deformation twinning and stacking fault formation in nanocrystalline Al [18–20], and the overall picture is consistent with post mortem TEM observations [15,67] and in situ X-ray diffraction experiments [14], which indicate that permanent dislocation networks are not built up during plastic deformation. Below 10–20 nm dislocation mechanisms become less probable and GB mechanisms such as sliding or rotation may take over, as forecast by MD simulations [7] and may be shown by partially convincing TEM experiments [9,58,60,75].

The micro-tensile results reported earlier [71] and the in situ experiments conducted in this study underscore the dramatic effect that microstructural instabilities have on the mechanical response of submicron free-standing nanocrystalline Al films. The mechanical behavior of these structures appears to not only be different than that of microcrystalline metals but dynamic as well. The in situ observations outlined in this manuscript reveal a far more complex picture than is traditionally espoused. Dislocations were observed to glide and interact in very small grains (Fig. 8) and evidence of massive and abnormally fast GB motion was uncovered in grains that were much larger than 100 nm (Fig. 5). It is also worth noting that these large grains initially experienced grain growth and then started deforming by classical dislocation processes once the grains reached a critical size. A direct implication of these observations is the fact that the grain size of nc-metals is not static but is prone to evolve under mechanical stress and strain.

In situ experiments offer unique insight into such evolution but are often influenced by the effect of the free surfaces on microstructural evolution and deformation processes. In the current study, the influence of specimen geometry was mitigated by the fact that the in situ experiments were carried out on the same nc-Al thin films that were used in the micro-tensile experiments conducted by Gianola et al. [71]. In both cases the films were deformed at room-temperature. Subtle differences lie in the strain rates, which were lower and continuous in the micro-tensile experiments, and the fact that pre-cracks concentrated the stress in the in situ samples. Discontinuous grain growth was observed in both cases and grain growth exceeded the film thickness. The grain growth cannot be attributed to the in situ nature of the experiments because similar or even greater grain growth was observed in the micro-tensile
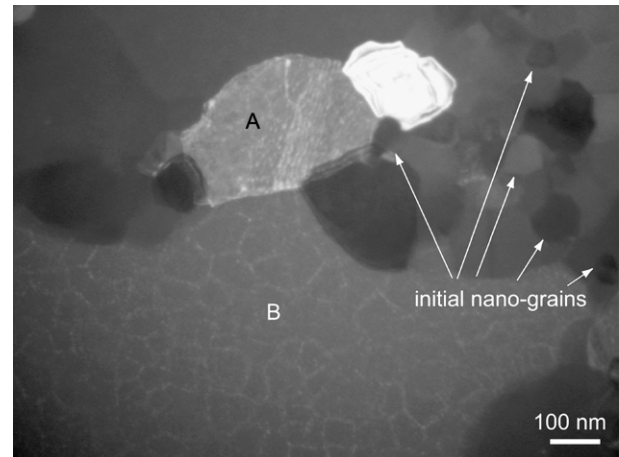

Fig. 9. Post mortem TEM picture taken on a micro-tensile strained film [71]. Note the very large grains (A and B) that have grown in the sea of initially nano-sized grains.

tested specimens, as exemplified by Fig. 9. This figure was taken using a plastically deformed 180 nm thick Al film whose as-deposited microstructure was homogeneous with an average initial grain size of 40 nm. After 2% deformation the microstructure contains very large grains in a sea of small neighboring grains (Fig. 9). These large grains (A and B) were found to be essentially dislocation-free, suggesting that a GB migration mechanism similar to the one in Fig. 5 took place. A light residual maze-like contrast was noted in grain B; the faint lines have the same approximate dimensions as the initial grain size and could be related to the level of impurities in the sample, as introduced and systematically studied by varying the background pressure during vapor deposition [76]. A critical concentration of dopants was consequently observed that was necessary for stabilizing the GBs during tensile testing. Post mortem observations and in situ X-ray diffraction of specimens taken to higher levels of strain indicate a lack of dislocation storage in the early stages of deformation followed by an invasion of the large grains with dislocations as deformation proceeds [71]. In this way, the post mortem and in situ observations lead to the same conclusions: that nc-Al films undergo significant discontinuous grain growth as a result of tensile loading, that this grain growth precedes dislocation activity, and that micro-scale dislocation processes are possible in the grains that have sufficiently grown.

Grain growth has also been observed under micro-indentations of nc-Cu [62,73] and in repeatedly indented nc-Ni [63], compressively deformed nc-Ni [77], and tensile strained Ni–Fe and Co–Pd alloys [64,65]. The fact that these specimens exhibit tensile and compressive ductility far exceeding that normally associated with nc-metals has led some to suggest that the improved ductility recently reported for dense nc-metals [78,79] may find its source in this grain growth (see below). Several studies, however, do not report grain growth but mainly grain rotation (see for instance Ref. [80]), which is surprising since grain

rotation is a known cause of grain growth by crystalline alignment of neighboring grains (see Refs. [5,8]).

Early in situ observations of grain-boundary motion in nc- and ufg-Al, referred to as "strain-induced coarsening" [81,82], also call into question the strain- versus stress-assisted nature of grain growth. The plot in Fig. 2d shows a clear correlation between grain growth and crack tip opening or strain, while Figs. 5 and 6 demonstrate the contrary: rapid GB motion during a non-straining period and back-and-forth motion of a GB under unidirectional loading. In fact, most of the observations made in this study suggest that the primary grain growth is stress-assisted. In all in situ experiments, primary grain growth was found to be ahead of the crack tip, that is, in the zone fully affected by the stress but very slightly strained. Fig. 2 illustrates a secondary grain growth process that happens through dislocation-mediated processes in already grown grains. Combining post mortem (Fig. 9, [71]) with the in situ experiments conducted for in this study suggests that stress-assisted grain growth is the dominant mechanism. This view is consistent with recently quantified observations of grain growth around stress concentrators in micro-tensile specimens, and compressed nc-Cu [74].

In the in situ experiments, grain growth was observed to occur at very different rates, suggesting different mechanisms. Rapid grain growth was observed to take place by the rapid motion of the GB (Figs. 5 and 6) or by the coalescence of closely oriented grains as in Fig. 7. This mechanism is very similar to the one invoked by Sergueeva and coworkers [75]. The coalescence noted in Fig. 7 is clear because dark field imaging produced images whose contrast and intensity are orientation-related. To appear in the same image, the orientation of two grains has to be within a few degrees. The fact that neighboring regions are successively lit up suggests that these region represent grains that have rotated into alignment with their neighbors. Going beyond this statement and quantifying the relative rotation or deformation of each superimposed grain, especially at the speed seen here, was not feasible in the current study.

Observations of rapid grain growth associated with very fast GB motion were entirely unexpected, and they are not consistent with "traditional" DIGM processes involving atomic diffusion to reduce GB curvature [27,83]. Several authors have measured the mobility of GB (see Ref. [84] for a review) and reported that GB motion occurs by a thermally activated process, promoted by an applied stress, with an energy of migration that is very close to that of either GB or bulk self-diffusion [38,42]. For instance, Li and coworkers [43] have calculated the mobility of a low-angle GB in stressed Zn bicrystals and found an activation energy of 90 kJ mol^{-1}, which corresponds to that of Zn self-diffusion. Similarly, extensive experimental work has been performed by Gottstein, Winning and co-workers on GB mobilities in Al bicrystals [38,39,41,42,85,86], and the mobility of their boundaries adhere to a thermally activated form

$$m = m_0 \exp(-E_m/kT) \qquad (2)$$

where m_0 is the pre-exponential factor and E_m the activation energy for grain-boundary migration. These authors have reported a clear transition between the activation energies for the migration of low- and high-angle GB. Depending on the GB considered, this transition occurs at around 8–15° for tilt boundaries and the activation energy is typically about 110–130 kJ mol^{-1} for low-angle GB and about half that (65–70 kJ mol^{-1}) for high-angle GB. These migration energies are comparable with volume and GB diffusion energies for pure Al (142 and 84 kJ mol^{-1}, respectively) [26]. Over the temperature range of 473–673 K, high-angle boundaries were reported to have a higher mobility than low-angle boundaries. The pre-exponential factors range from 0.4 to 0.8 m s^{-1} MPa^{-1} for high-angle GB and from 1500 to 80,000 m s^{-1} MPa^{-1} for low-angle boundaries.

We do not know the nature of the mobile GBs observed in the present in situ work, but we can compare their mobility to the more mobile planar tilt GBs in Al bicrystals. Those are of <1 0 0> type. At room-temperature, their mobility is 2×10^{-6} nm s^{-1} MPa^{-1} for low-angle and 1.5×10^{-3} nm s^{-1} MPa^{-1} for high-angle boundaries (pre-exponential factor of 79,500 and 0.44 m s^{-1} MPa^{-1} and migration energies of 113 and 66 kJ mol^{-1} for low- and high-angle GB, respectively) [86]. Applying the same stress (between 100 and 200 MPa) as previously found in the present in situ and previous micro-tensile tests [71] lead to GB velocities ranging between 2×10^{-5} and 0.3 nm s^{-1}, if we assume that the orientation with respect to the stress tensor is optimal. This corresponds fairly well to the average low GB velocities observed in situ (0.1 nm s^{-1} in Fig. 4 and corresponding paragraph). However, the random orientation of GBs with respect to the applied stress in the present work [39] and their highly curved shape should lead to an overall lower mobility since curved boundaries have higher migration energies than planar ones [85]. Moreover, most of the boundaries observed in the present work have a connection to the surface which is known to impede their mobility because of grooving [45] and intrinsic atomic rearrangement [87]. The residual contrast seen in Fig. 9 may be a signature of the surface grooves left behind by the initial GB that subsequently detached under the applied stress and moved to absorb the surrounding grains. Finally, if we take in account the much lower mobility of other types (<1 1 1> and <1 1 2>) of planar tilt GBs [42], it appears that the average velocities observed in situ in nc-Al are clearly above those measured in bicrystals and attributed to DIGM processes. The fastest events (30–50 nm s^{-1} in Figs. 5 and 6) are orders of magnitude above mobilities predicted from Al bicrystals data and clearly call for a different GB displacement mechanism.

Several hypotheses can be explored to explain the unusually high GB velocities that have been observed. If a diffusion mechanism is involved, the activation energy would have to be very low, and this is probably the case for the slower events. MD simulations [7,88,89] have suggested that "stress-induced" GB diffusion may operate at

room-temperature in specimens with very small grain sizes, but the level of stress computed in these simulations is much higher than those measured in the present experiments. The atomic shuffling model of Babcock and Balluffi [30] could also be used to explain some of the features observed here. The sometimes observed jerky motion of GBs is compatible with the hypothesis of a kink-type propagation of reorienting cells only at the GB interface. This short-range diffusion-based model could also explain unusually high GB mobility, i.e. low migration energy, as compared to long-range diffusion, such as in Coble creep. Finally, the fact that some small grains resist the expansion of larger one suggests the existence of "hard" orientations (see Fig. 9) for which atomic shuffling is not favorable. Further investigation into the applicability of this model is warranted.

Another route to be considered is the model of stress-assisted GB motion that was recently put forth by Cahn and coworkers [35,37] that is based on the shear-coupled motion of GB. The military nature of GB motion as a result of this mechanism removes the dependence on diffusion and allows for very fast athermal GB migration. The Frank–Bilby equation that determines the character of the boundary and thus the direction of the shear, leads to two distinct branches, positive or negative, for the coupling factor. A consequence of this bifurcation is the fact that a boundary that changes character as it moves could actually move from one branch to the other and result in a GB motion that reverses under the same constant applied shear. The observed back-and-forth motion of the GB in Fig. 6 could be an illustration of this mechanism. Winning's bicrystal results [40] have also been interpreted in terms of stress-coupled grain-boundary migration, but the fact that applied stresses in the nc-Al samples are much higher than can be realized in coarse-grained Al may be used to explain why the stress-coupling and GB migration is more general in the nc-Al. The faceted shape of the growing grains (see for example Figs. 4 and 5) and the discontinuous nature of the grain growth observed throughout this study are both consistent with the idea that some boundaries would couple more favorably than others. Detailed comparison with this model would require thorough orientation of the grains on both sides of the moving GB, which is practically impossible for very small grains, but could in principle be realized for larger ones, such as those in Fig. 5. The in situ stage and conditions used in the present study were not amenable to these measurements but parallel efforts are warranted and underway.

5. Summary and conclusions

Nanocrystalline Al submicron films with initial average grain sizes of 40–90 nm have been tensile tested in situ in a TEM at room-temperature. The following summary and conclusions have been drawn from these dynamic and post mortem TEM observations:

- Dynamic observations of stress-assisted grain growth have been recorded in these nc-Al films. This grain growth precedes dislocation activity, involves GB migration and grain coalescence, and results in discontinuous grain growth, where a limited number of preferential grains grow to be several times the film thickness (180/380 nm) and are then surrounded by a sea of nanocrystalline grains that have maintained their initial dimensions.
- This grain growth was observed to occur preferentially under the applied load in the highly stressed regions ahead of crack tips. No growth was observed in regions away from the cracks or without the application of load. The in situ observations that stress concentrations at crack tips lead to preferential grain growth and crack tip blunting has profound implications for the fracture toughness of nanocrystalline materials.
- Despite the presence of free surfaces, very large GB velocities exceeding $200 \ nm \ s^{-1}$ for collapsing small grains and larger than $30 \ nm \ s^{-1}$ in growing grains were observed. This grain-boundary migration could be a new plastic relaxation mechanism in nc-Al since neither diffusion nor dislocation-based models can fully account for the observed GB speed at room-temperature.
- Parallel plasticity processes were observed and taken as an indication that the notion of uncovering and identifying independent grain-size-dependent deformation mechanisms may be overly simplistic. Pure GB processes (without GB/dislocation interaction) were observed to be active in both small nanocrystalline and large grown grains. Extensive dislocation motion, tangling and sub-grain formation was generally restricted to larger grains that had grown to a critical size, but individual dislocation activity was observed in grains as small as 40–50 nm.

Acknowledgement

Appendix A. Supplementary material

Supplementary data associated with this article can be found, in the online version, at doi:10.1016/j.actamat.2008.03.032.

References

[1] Hall EO. Proc Phys Soc Sect B 1951;64:747.
[2] Petch NJ. J Iron Steel Inst 1953;174:25.
[3] Hemker KJ, Sharpe WNJ. Ann Rev Mater Res 2007;37:93.
[4] Chen M, Ma E, Hemker KJ. Mechanical behavior of nanocrystalline metals. In: Gogotsi Y, editor. Nanomaterials handbook. CRC Press, Taylor and Francis; 2006.
[5] Meyers MA, Mishra A, Benson DJ. Prog Mater Sci 2006;51:427.
[6] Van Swygenhoven H, Weertman JR. Mater Today 2006;9:24.
[7] Van Swygenhoven H, Derlet P. Phys Rev B 2001;64:224105.

[8] Ma E. Science 2004;305:623.

[9] Shan Z, Stach EA, Wiezorek JMK, Knapp JA, Follstaedt DM, Mao SX. Science 2004;305:654.

[10] Coble RL. J Appl Phys 1963;34:1679.

[11] Yamakov V, Wolf D, Phillpot SR, Gleiter H. Acta Mater 2002;50:61.

[12] Van Swygenhoven H, Derlet PM, Hasnaoui A. Phys Rev B 2002;66:024101.

[13] Liao XZ, Zhou F, Lavernia EJ, Srinivasan SG, Baskes MI, He DW, et al. Appl Phys Lett 2003;83:632.

[14] Budrovic Z, Van Swygenhoven H, Derlet PM, Van Petegem S, Schmitt B. Science 2004;304:273.

[15] Kumar KS, Suresh S, Chisholm MF, Horton JA, Wang P. Acta Mater 2003;51:387.

[16] Van Swygenhoven H, Derlet PM, Froseth AG. Acta Mater 2006;54:1975.

[17] Yamakov V, Wolf D, Phillpot SR, Mukherjee AK, Gleiter H. Nat Mater 2002;1:45.

[18] Chen M, Ma E, Hemker KJ, Sheng H, Wang Y, Cheng X. Science 2003;300:1275.

[19] Liao XZ, Zhou F, Lavernia EJ, He DW, Zhu YT. Appl Phys Lett 2003;83:5062.

[20] Liao XZ, Zhao YH, Srinivasan SG, Zhu YT, Valiev RZ, Gunderov DV. Appl Phys Lett 2004;84:592.

[21] Van Swygenhoven H, Derlet PM, Froseth AG. Nat Mater 2004;3:399.

[22] Schiotz KW, Jacobsen KW. Science 2003;301:1357.

[23] Hillert M. Scripta Metall 1983;17:237.

[24] Brechet YJM, Purdy GR. Acta Metall 1989;37:2253.

[25] Balluffi RW, Cahn JW. Acta Metall 1981;29:493.

[26] Frost HJ, Ashby MF. Deformation mechanisms maps. Oxford: Pergamon Press; 1982.

[27] Atkinson HV. Acta Metall 1988;36:469.

[28] Merkle KL, Thompson LJ. Mater Lett 2001;48:188.

[29] Babcock SE, Balluffi RW. Acta Metall 1989;37:2357.

[30] Babcock SE, Balluffi RW. Acta Metall 1989;37:2367.

[31] Humphrey PH. Special angle grain boundaries. In: Chadwick GA, Smith DA, editors. Grain boundary structure and properties. London, New York, San Francisco: Academic Press; 1976. p. 39.

[32] Caillard D, Martin JL. Acta Metall 1982;30:791.

[33] Molodov DA, Ivanov VA, Gottstein G. Acta Mater 2007;55:1843.

[34] Cahn JW, Taylor JE. Acta Mater 2004;52:4887.

[35] Cahn JW, Mishin Y, Suzuki A. Philos Mag 2006;86:3965.

[36] Suzuki A, Mishin Y. Mater Sci Forum 2005;502:157.

[37] Cahn JW, Mishin Y, Suzuki A. Acta Mater 2006;54:4953.

[38] Winning M, Gottstein G, Shvindlerman LS. Acta Mater 2002;50:353.

[39] Gottstein G, Molodov DA, Shvindlerman LS, Srolovitz DJ, Winning M. Curr Opin Solid State Mater Sci 2001;5:9.

[40] Winning M. Philos Mag 2007;87:5017.

[41] Winning M, Gottstein G, Shvindlerman LS. Acta Mater 2001;49:211.

[42] Winning M, Gottstein G, Shvindlerman LS. Mater Sci Eng A 2001;317:17.

[43] Li CH, Edwards EH, Washburn J, Parker ER. Acta Metall 1953;1:223.

[44] Bainbridge DW, Li CH, Edwards EH. Acta Metall 1954;2:322.

[45] Polcarova M, Bradler J, Jacques A, Lejcek P, George A, Ferry O. J Phys D: Appl Phys 2003;36:A98.

[46] Weiss S, Gottstein G. Mater Sci Eng A 1998;256:8.

[47] Molodov DA, Konijnenberg P, Hu W, Gottstein G, Shvindlerman LS. Scripta Mater 2001;45:229.

[48] Gemperlova J, Jacques A, Gemperle A, Vystavel T, Zarubova N, Janecek M. Mater Sci Eng A 2002;324:183.

[49] Caillard D. Philos Mag 1985;51:157.

[50] Ferry M, Humphreys FJ. Acta Mater 1996;44:1293.

[51] Czubayko U, Sursaeva VG, Gottstein G, Shvindlerman LS. Acta Mater 1998;46:5863.

[52] Farkas D, Froseth A, Van Swygenhoven H. Scripta Mater 2006;55:695.

[53] Hahn H, Mondal P, Padmanabhan KA. Nanostruct Mater 1997;9:603.

[54] Hasnaoui A, Van Swygenhoven H, Derlet PM. Acta Mater 2002;50:3927.

[55] Haslam AJ, Yamakov V, Moldovan D, Wolf D, Phillpot SR, Gleiter H. Acta Mater 2004;52:1971.

[56] Yamakov V, Moldovan D, Rastogi K, Wolf D. Acta Mater 2006;54:4053.

[57] Wolf D, Yamakov V, Phillpot SR, Mukherjee A, Gleiter H. Acta Mater 2005;53:1.

[58] Chen M, Yan X. Science 2005;308:356c.

[59] Li H. Adv Eng Mater 2005;7:1109.

[60] Shan Z, Stach EA, Wiezorek JMK, Knapp JA, Follstaedt DM, Mao SX. Science 2005;308:356d.

[61] Schwaiger R. Deformation of nanostructured materials: insights from experimental observations. The International Society for Optical Engineering; 2005.

[62] Zhang K, Weertman JR, Eastman JA. Appl Phys Lett 2004;85:5197.

[63] Schwaiger R, Suresh S. Cyclic contact deformation of nanocrystalline Ni. TMS Annual Meeting. San Antonio; 2006.

[64] Fan GJ, Fu LF, Qiao DC, Choo H, Liaw PK, Browning ND. Scripta Mater 2006;54:2137.

[65] Fan GJ, Wang YD, Fu LF, Choo H, Liaw PK, Ren Y, Browning ND. Appl Phys Lett 2006;88:171914.

[66] Agnew SR, Elliott BR, Youngdahl CJ, Hemker KJ, Weertman JR. Mater Sci Eng A 2000;285:391.

[67] Legros M, Elliott BR, Rittner MN, Weertman JR, Hemker KJ. Philos Mag A (Phys Condens Mat: Struct Defects Mech Prop) 2000;80:1017.

[68] Gianola D, Legros M, Hemker KJ, Sharpe WJ. TMS Lett 2004:149.

[69] LaVan DA, Sharpe WNJ. Exp Mech 1999;39:210.

[70] Sharpe WNJ, Pulskamp J, Mendis BG, Eberl C, Gianola DS, Hemker KJ. Tensile stress–strain curves of gold films. In: Proceedings of the ASME Int. Mech. Eng. Congr. Exp., Chicago; 2006. p. 13290.

[71] Gianola DS, Van Petegem S, Legros M, Brandstetter S, Van Swygenhoven H, Hemker KJ. Acta Mater 2006;54:2253.

[72] Gianola DS, Warner DH, Molinari JF, Hemker KJ. Scripta Mater 2006;55:649.

[73] Zhang K, Weertman JR, Eastman JA. Appl Phys Lett 2005;87:061921.

[74] Brandstetter S, Zhang K, Escuadro A, Weertman JR, Van Swygenhoven H. Scripta Mater 2008;58:61.

[75] Sergueeva AV, Mara NA, Krasilnikov NA, Valiev RZ, Mukherjee AK. Philos Mag 2006;86:5797.

[76] Gianola DS, Mendis BG, Cheng XM, Hemker KJ. Mater Sci Eng A 2008;483–484:637.

[77] Pan D, Kuwano S, Fujita T, Chen MW. NanoLetters 2007;7:2108.

[78] Wang Y, Chen M, Zhou F, Ma E. Nature 2002;419:912.

[79] Champion Y, Langlois C, Guerin-Mailly S, Langlois P, Bonnentien J-L, Hytch M-J. Science 2003;300:310.

[80] Noskova NI. J Alloys Compd 2007;434–435:307.

[81] Jin M, Minor AM, Stach EA, Morris JJW. Acta Mater 2004;52:5381.

[82] Morris JJW, Jin M, Minor AM. Mater Sci Eng A 2007;462:412.

[83] Brechet YJM, Purdy GR. Scripta Mater 2006;54:2009.

[84] Gottstein G, Schvindlerman LS. Grain boundary migration in metals. Boca Raton, USA: CRC Press; 1999.

[85] Winning M. Acta Mater 2003;51:6465.

[86] Winning M, Rollett AD. Acta Mater 2005;53:2901.

[87] Zhou L, Zhang H, Srolovitz DJ. Acta Mater 2005;53:5273.

[88] Van Swygenhoven H, Spaczer M, Caro A, Farkas D. Phys Rev B 1999;60:22.

[89] Zhu B, Asaro RJ, Krysl P, Zhang K, Weertman JR. Acta Mater 2006;54:3307.